J. D. Swalen R. Santo M. Tacke J. Fischer

# Properties of Polymeric Thin Films by Integrated Optical Techniques

Abstract: We report an innovative procedure for taking measurements using integrated optical techniques on a number of polymers fabricated into thin film form and used as optical waveguides. Refractive index (including anisotropy), absorption and scattering, and film thickness have been determined by light guiding properties. Techniques for film preparation, including doctor blading, dipping, horizontal flowing, and spinning, are also discussed. The polymers studied are poly(methyl methacrylate), poly(vinyl-formal), polyacrylonitrile, poly(vinyl alcohol), poly(vinyl pyrrolidone), poly(vinyl benzoate), and polystyrene.

#### Introduction

Integrated optics, the transmission of light in guided waves through film, is an active area of research and development because of its potential use in communications and optical signal processing [1-5]. Many bulk optical properties have now been reproduced and duplicated in thin film form, some with even a few additional phenomena and effects. A variety of inorganic and organic materials used to fabricate passive thin film wave guides have been investigated [4]. Some of the inorganic compounds used are zinc oxide and sulfide, tantalum oxide, niobium oxide, and sputtered glass: the organic materials considered are reported in Table 1.

We have been using some of these polymeric films for spectroscopic and electrochromic measurements of organic monolayers in or on films. In doing so we have investigated their optical properties and report our results on their refractive indices, including anisotropy as a function of wavelength. Measurements of absorption and scattering losses are also reported. It will become clear that integrated optics is an accurate and quick method for determining these optical constants of the polymer films [4, 6-11].

# Methods of film preparation

In Table 1 we list a number of methods of fabrication. Briefly these are described as follows: a) The horizontal flow method involves covering a slide (fused silica in our case) with a solution of a polymer from a syringe, bringing the slide to a vertical position to drain off the excess solution, and then returning it to a horizontal position for drying. (A similar technique involves dipping

as a first step.) b) Spinning begins by adding a few drops of polymer solution, at a concentration of around 10 percent, to a slide on a spinner and then subsequently spinning it at approximately 1000 rpm. c) Doctor blading involves moving a knife edge along a substrate to spread out the solution. The separation between the knife edge and substrate, called the "wet gap," is 40-60  $\mu$ m and can be adjusted by micrometer screws against teflon riders in contact with the substrate. A stepping motor drives a plate with a vacuum chuck holding the substrate at about 1 mm/s past the knife edge; metal pads in front of and behind the film with thicknesses equal to that of the substrate serve to catch the beginning and final puddle of polymer solution resulting in more uniform films over the substrate.

Generally, thinner films are produced by spinning than by the horizontal flow, dipping, or doctor blading techniques. Each of the spreading techniques, however, tends to produce an anisotropy in refractive index. This means that the refractive index in the plane of the film is different from that perpendicular to it. We did not attempt to measure any anisotropy within the plane though some probably exists there too, specially for doctor blading where one might expect some flow birefringence. (We tend to favor the doctor blading technique because it appeared in our experiments to be the most controllable and reliable method, and in the work reported here we used doctor blading almost exclusively.)

For the above mentioned techniques the solvents used were water for both poly(vinyl alcohol), and poly(vinyl pyrrolidone) and chlorobenzene or dimethyl formamide

Table 1 Typical polymers used in integrated optical films and devices.

Polymer	n	Method of fabrication	Reference	
poly(urethane)	1.55 – 1.57	horizontal flow		
poly(urethane)	1.525	spread on water surface	32	
epoxy	1,581	horizontal flow	31	
photoresist	1.615	horizontal flow	31, 33	
poly(methyl-methacrylate) (PMMA)	1.486 - 1.490	spinning	14, 33, 34, 36	
styrene-acrylonitride copolymer	1.556-1.563	horizontal flow	12	
poly(trimethylsilane) (TRMS)	1.567	rf discharge polymerization	14-18	
poly(vinyltrimethyl-silane) (VTMS)	1.539	rf discharge polymerization	14 – 18	
polystyrene	1.58 - 1.60	horizontal flow	33, 34, 35	
poly(vinyl alcohol)	1.52	doctor blade	13	
poly(vinyl-formal)	1.51	doctor blade	13	
poly(vinyl carbazole)	1.68	doctor blade	13	

for the other polymers studied. A high boiling solvent, i.e. one that evaporates slowly, is preferred to avoid crazing the surface. A trace of silicon oil [12] or drying in the presence of solvent vapor [13] have both been shown to be advantageous. All methods, but especially spinning, require a solvent that thoroughly wets the substrate. Oven drying at 330 K is typical to remove any remaining solvent.

A final method, d) rf discharge polymerization, involves adding monomers to an rf discharge chamber containing substrates. A highly cross linked film of some polymer mixture results, and the composition is a complicated function of the conditions and the monomer used [14-18].

## Integrated optics

Figure 1 shows a cross-section schematic of a thin film waveguide, where a laser beam is transmitted into and out of the guide by two prism couplers. The optical, electric, and magnetic fields decay into the lower refractive index regions of the substrate (fused silica) and the superstrate (air). Figure 2 shows the intensity of the optical field (proportional to E<sup>2</sup>, the square of the electric field intensity) of the light in a guide for a typical film of poly(vinyl alcohol). Four different modes are plotted; they are numbered by a value m, which is the number of electromagnetic nodes that occur within the polymer film. Each mode propagates with a slightly different effective refractive index, which is defined as the ratio of the velocity of propagation in free space to that of the bound wave. By a ray optics approach we can envision the ray bouncing back and forth between the two total internally reflecting interfaces with evanescent waves in the superstrate and substrate and phase shifts being experienced at both of these interfaces. Different modes have different wave front angles and to select a different mode one merely changes the coupling angle of

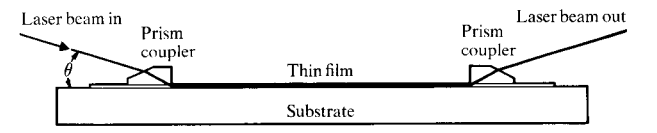


Figure 1 Schematic for prism coupling into a thin film light wave guide.

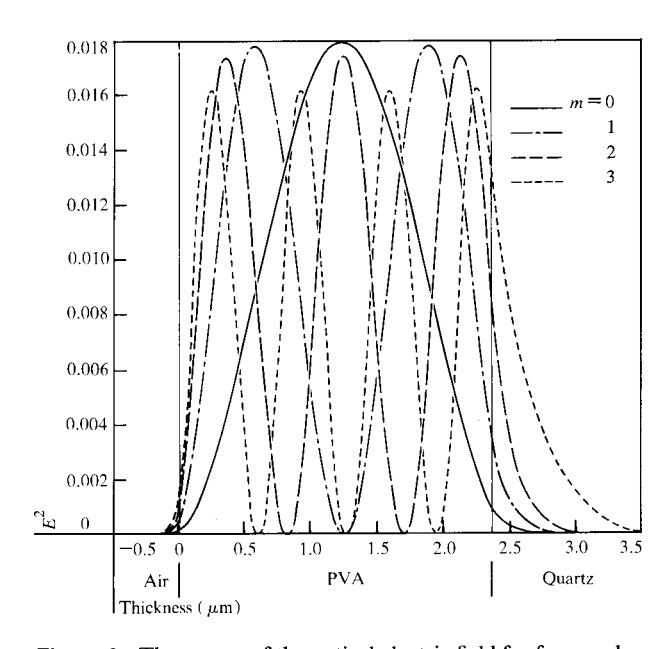
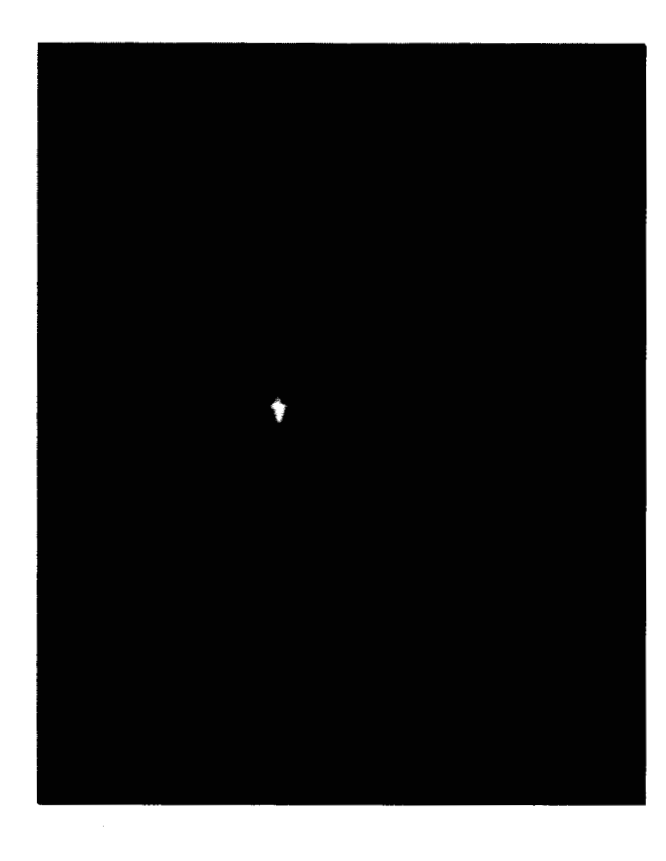


Figure 2 The square of the optical electric field for four modes across a film 2.35  $\mu m$  thick.

the laser beam into the input prism by rotating the film and substrate around an axis perpendicular to the plane of the figure. The light is coupled out at distinct angles





m lines with angle

Figure 3 Photograph of "m" lines.

too. As shown in Fig. 3, photographic plates positioned behind the outcoupling prism show the patterns when the incident angle (Fig. 1) is set to propagate the m = 1mode. Note that other modes are weakly observed because of surface roughness and multiple couplings. Furthermore, for the longer wavelength red (helium-neon) laser, the film can only support three modes. The m=3mode is beyond cutoff and hence missing. Figure 4 gives a plot of the intensity of the out-coupled beam vs the rotation angle of the input beam relative to the prism base utilizing the arrangement shown in Fig. 1. Coupling, which must be weak to avoid angular error, occurs only at certain angles [4]. Furthermore, the two traces shown are for the polarization of the transverse magnetic (TM) and transverse electric (TE) modes. Both are separately coupled by choosing the appropriate polarization of the input beam.

The dispersion relations are found by solving Maxwell's equations [19-23]. Assuming an oscillatory propagating solution in the film (labeled 2) in Eq. (1) and exponentially decaying fields outside the film, i.e. in the substrate (labeled 3) and superstrate (labeled 1), one obtains the eigenvalue equation in the notation of Polky & Mitchell [24] by matching both the H and E fields at the interface.

$$\tan^{-1}\frac{K_1}{K_2} + \tan^{-1}\frac{K_3}{K_2} + m\pi = U_2 t, \tag{1}$$

where

$$\begin{split} K_i &= U_i/\gamma_i = (|\beta^2 - n_i^2 k^2|)^{\frac{1}{2}}/\gamma_i, \\ \gamma_i &= 1 \text{ for TE} \\ &= n_i^2 \text{ for TM}, \\ k &= 2\pi/\lambda, \end{split}$$

and t is the film thickness, and  $n_i$  is the refractive index for the ith layer. This can also be understood by a ray optics approach. The first two terms of Eq. (1) are the mentioned phase shifts at the interfaces and their combination with the phase shift from propagation perpendicular to the film  $(U_2t)$  must be a multiple of  $2\pi$ . (Note: a factor of 2 has been divided out in Equation 1.) Furthermore when coupling occurs, the effective index  $\beta/k$  in the direction of propagation is related to the coupling angle  $(\theta)$  to the prism.

$$\beta/k = n_{\rm p} \sin \left[ \alpha + \sin^{-1} \left( \frac{\cos (\alpha + \theta)}{n_{\rm p}} \right) \right],$$
 (2)

where  $\alpha$  is the acute angle of the prism and  $n_{\rm p}$  is the refractive index.

This effective index  $\beta/k$  takes on values only between  $n_2$  and  $n_3$  and typical solutions of Eq. (1) are shown in Fig. 5 where film thickness is plotted vs  $\beta/k$ . Refractive index and thickness can thus be determined accurately

170

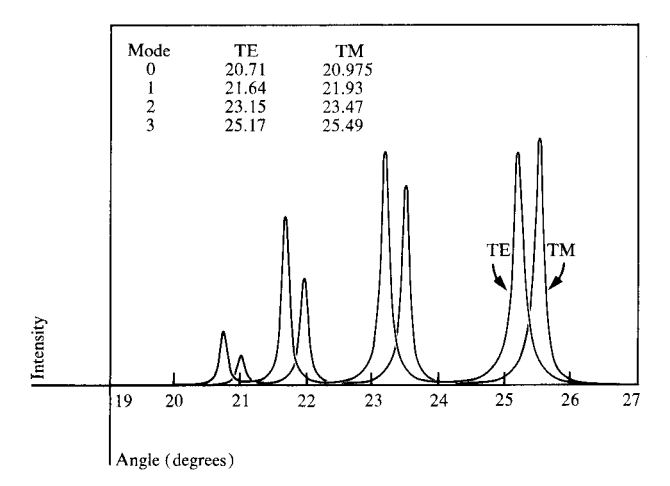


Figure 4 Propagation of light intensity vs coupling angles, i.e. the "synchronous angles" for TE and TM.

but two or more guided modes are needed to simultaneously determine both. One generally works with films approximately in the 1  $\mu$ m to 5  $\mu$ m thickness range. The lower limit results from the fact that a film supports only a finite number of modes and, if too thin, may have only one mode or even none. The upper limit results from the fact that thick films support too many modes, making mode assignment difficult and reducing accuracy.

Films thinner than 1  $\mu$ m can be analyzed in combination with other films; we have used sputtered glass films, relabeled 3 in Eq. (3), on the fused silica substrates, relabeled 4. The term  $K_3$  in Eq. (1) now becomes

$$K_3 \to K_3 \left\{ \frac{\frac{K_4}{K_3} - \tan U_3 t_3}{1 + \frac{K_4}{K_3} \tan U_3 t_3} \right\}.$$
 (3)

For some modes this structure may act as a guide, though one of the layers (either 2 or 3) may be beyond cutoff because its refractive index is below  $n_{\rm eff} = \beta/k$  while the index of the other layer is still above. For the non-guiding-layer the tangent function in the braces of Eq. (3) then becomes a hyperbolic tangent. For example, with layer 3 below cutoff the bracket becomes

$$\left\{ \frac{\frac{K_4}{K_3} + \tanh \ U_3 t_3}{1 + \frac{K_4}{K_2} \tanh \ U_3 t_3} \right\}.$$
(4)

Figure 6 shows an example of the  $E^2$  optical field for the case with both layers guiding (solid curve) and for the case with only one layer guiding (dashed curve).

An experimental APL computer program uses Eqs. (1-4) to calculate the "best" values for thickness and refractive index.

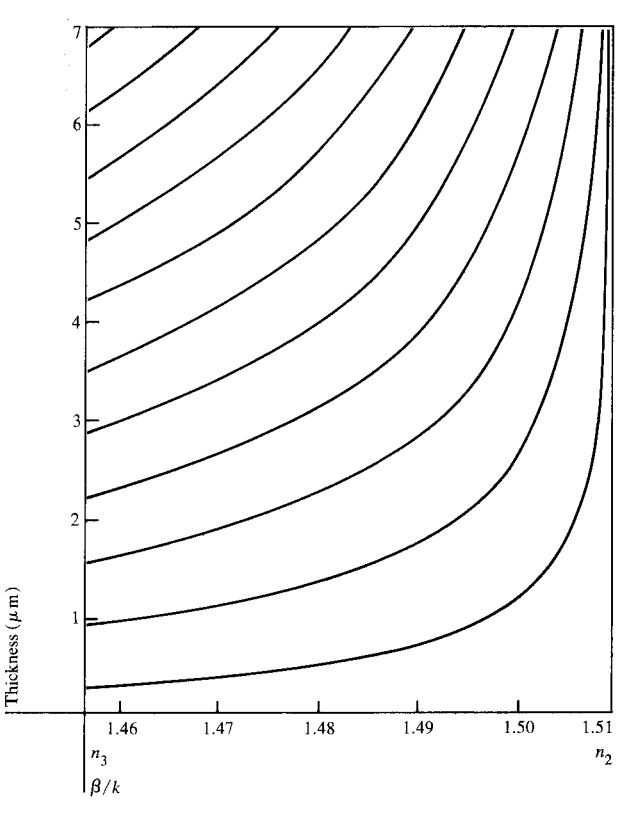


Figure 5 Film thickness for a number of modes vs effective refractive index for films with  $n_2 = 1.51$  on quartz which has refractive index  $n_3 = 1.457$ .

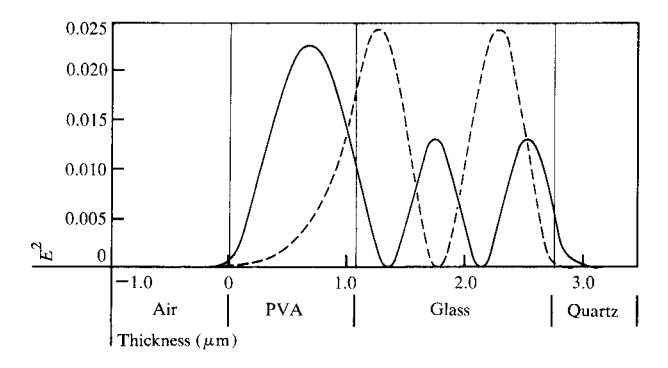


Figure 6 Field pattern for two modes in a two-layered film of PVA and sputtered glass on quartz.  $E^2$  is in normalized units.

#### **Optical constants of polymers**

Using the doctor blading technique, we prepared a number of polymeric films 2 to 3  $\mu$ m thick and measured their modes at five different wavelengths approximately uniformly spaced but limited to the laser lines available. The dye laser was set to the sodium D lines (0.5892  $\mu$ m) to give an immediate comparison to other published

Table 2 Average refractive indices and anisotropy.

Polymer	Refractive index for various laser wavelengths					Anisotropy
	$\lambda = 0.6328$	$\lambda = 0.5892$	$\lambda = 0.5287$	$\begin{array}{c} \lambda = \\ 0.4880 \end{array}$	λ = 0.4579	
polystyrene	1.5845	1.5882	1.5939	1.6008	1.6075	-0.0037
poly(vinyl benzoate)	1.5636	1.5673	1.5742	1.5804	1.5874	$\pm 0.0002$
poly(vinyl pyrrolidone)	1.5247	1.5259	1.5302	1.5341	1.5370	-0.0029
poly(vinyl alcohol)	1.5145	1.5162	1.5195	1.5224	1.5251	0.0023
polyacrylonitrile	1.5115	1.5131	1.5161	1.5195	1.5227	-0.0012
poly(vinyl-formal)	1.5003	1.5016	1.5047	1.5076	1.5102	0.0037
poly(methyl methacrylate)	1.4856	1.4876	1.4915	1,4945	1.4964	$\pm 0.0002$

Table 3 Attenuation of light in selected films.

Polymer	Wavelength (μm)	Atteni (dB)	Thickness (µm)	
	(F* -7)	TE	TM	(James)
Poly(vinyl alcohol)	0.6328	1.25±0.05	0.65±0.05	2.75
	0.4416	$6.01\pm0.11$	$2.60\pm0.05$	2.75
Poly(vinyl-formal)	0.6328	$0.34\pm0.10$	$0.80\pm0.10$	4.31
Poly(vinyl pyrrolidone)	0.6328	$0.30\pm0.30$	$0.30\pm0.20$	3.46

<sup>\*</sup>For the m = 0 mode

Table 4 Refractive indices by molecular refractions.

Polymer	n (observed)	n (calculated)	n (Lange
eflon	1.350	1.348	1.329
ooly(vinyl acetate)	1.467	1.461	1.469
poly(methyl methacrylate)	1.490	1.493	1.503
ooly(vinyl-formal)	1.510	1.520	1.480
poly(ethylene)	1.510	1.507	1.519
ooly(chlorovinyl acetate)	1.513	1.514	1.513
ooly(vinyl alcohol)	1.516	1.525	1.540
poly(vinyl benzoate)	1.567	1.570	1.544
polystyrene	1.592	1.595	1.588

	Atomic refractions Our values	Lange	
C	4.206	2.418	
Н	0.161	1.1	
0—	1.567	1.64	
0=	0.438	2.211	
Cl	5.398	5,967	
F	0.331	1.1	
N	3.5	3.5	
C=C	<u>-</u>	1.73	

values. The other lines used were  $0.6328~\mu m$  from the helium neon laser and  $0.5287~\mu m$ ,  $0.488~\mu m$  and  $0.4579~\mu m$  from the argon ion laser. Table 2 and Fig. 7 show our results for the indices of refraction which do not depend on film thickness in our thickness range. A dispersion curve has been determined with a power series fit by the least-squares procedure,

$$n^2 - 1 = \sum_{n = -2}^{+2} a_n \lambda^n.$$
 (5)

The refractive index in the plane of the film as determined by the TE mode can be greater, smaller or equal to the refractive index perpendicular to the film as determined by the TM mode. We list, in Table 2, these observed differences under the column entitled anisotropies where  $n_{\rm TE}-n_{\rm TM}$  is tabulated. They tend to be, to a first approximation, wavelength insensitive. The very low values for poly(vinyl benzoate) and PMMA show the high accuracy of the technique. Figure 8 expands the ordinate scale for poly(vinyl alcohol) to show the anisotropy more clearly. It should be noted, however, that calculations with an anisotropy [11] required a modification of Eqs. (1), (3), and (4).

Measurements of the sum of absorption and scattering have been taken on a few films by measuring the drop in intensity of the scattered light along a track [4, 33]. For our films and path lengths of one cm this turned out to be a difficult experiment because many films are so good that little attenuation could be recorded. In Table 3 we give our values in dB/cm (divided by 4.3 to convert to absorption coefficient  $\alpha$  in cm<sup>-1</sup>).

If the various absorption frequencies of a material are known, the oscillator strengths  $f_i$  can then be obtained by fitting the Cauchy relation, Eq. (6), where N is the number of electrons, e is the electronic charge, m is the electronic mass and  $\gamma$  is related to the line width.

$$n^{2} = 1 + \sum_{i} \frac{4\pi N e^{2}}{m} \frac{f_{i}}{\omega_{j}^{2} - \omega^{2} + i\gamma\omega}.$$
 (6)

We measured the absorption of these films with a Cary-14 spectrometer and these spectra are plotted in Fig. 9. Limited to a shortest wavelength of about 190 nm, these data were not sufficient to evaluate the sum in Eq. (6). The vacuum ultraviolet absorption spectrum of polystyrene has, however, been measured by Partridge [25] and he observed bands at 80 nm and 195 nm; the latter we have also observed. By fitting our refractive indices to Eq. (6) with these wavelengths and no damping ( $\gamma = 0$ ) we arrived at a ratio of oscillator strengths of 11 for these two bands. An approximate integration of Partridge's spectrum gave a ratio a factor of two larger. A variety of reasons could cause this discrepancy, such as missing bands, errors in intensities, and the use of Eq. (6) without damping.

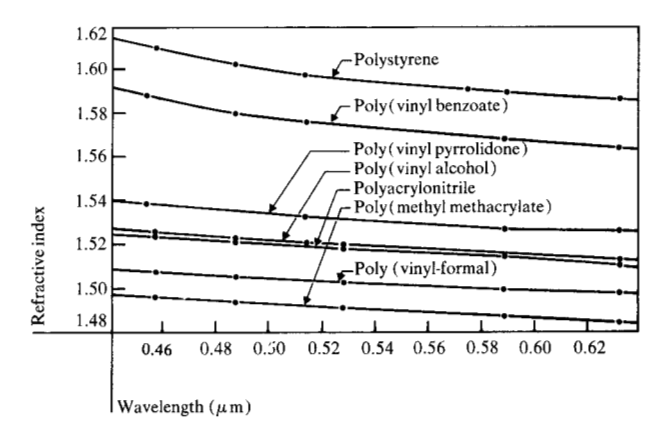


Figure 7 Refractive index vs wavelength in  $\mu$ m for a number of polymeric films measured.

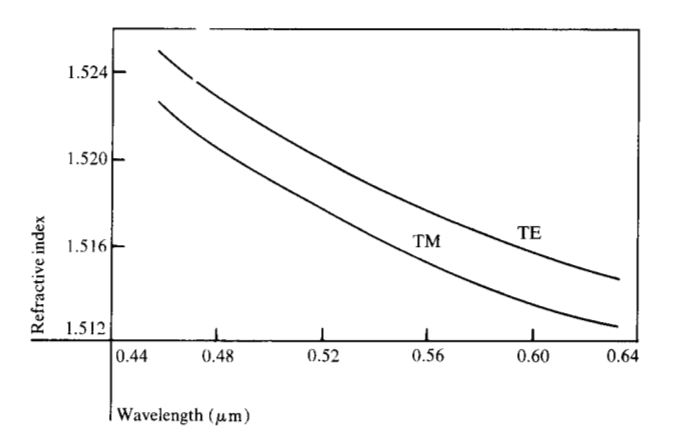


Figure 8 On an expanded ordinate the refractive index of a poly(vinyl alcohol) film is shown as a function of wavelength. TE modes have their polarization in the plane of the film and TM modes have theirs within a few degrees of being perpendicular to it.

Nevertheless, a crude agreement is obtained. Finally, the refractive indices n, of polymers can be fit with molecular refractions [R] to the Lorenz-Lorentz Eq. (7).

$$\frac{n^2 - 1}{n^2 + 2} \frac{M}{\rho} = [R] = \frac{4\pi N}{3} \sum_{i} N_i \alpha_i, \tag{7}$$

where M is the molecular weight and  $\rho$  is the density. N is Avogadro's number, and  $N_i$  is the number of ith units with atomic polarizability  $\alpha_i$ . By a least squares fit to the refractive indices of 31 polymers, using the bulk density and the molecular weight of a repeat unit, we obtained the results given in Table 4. Our set of atomic refractions are compared to those given for organic liquids [26]. The agreement is quite good for both; in fact, much better than one should expect. Pitzer [27] and Mills [28] discuss the difficulty of introducing and assigning consistent values for bond anisotropies and properly

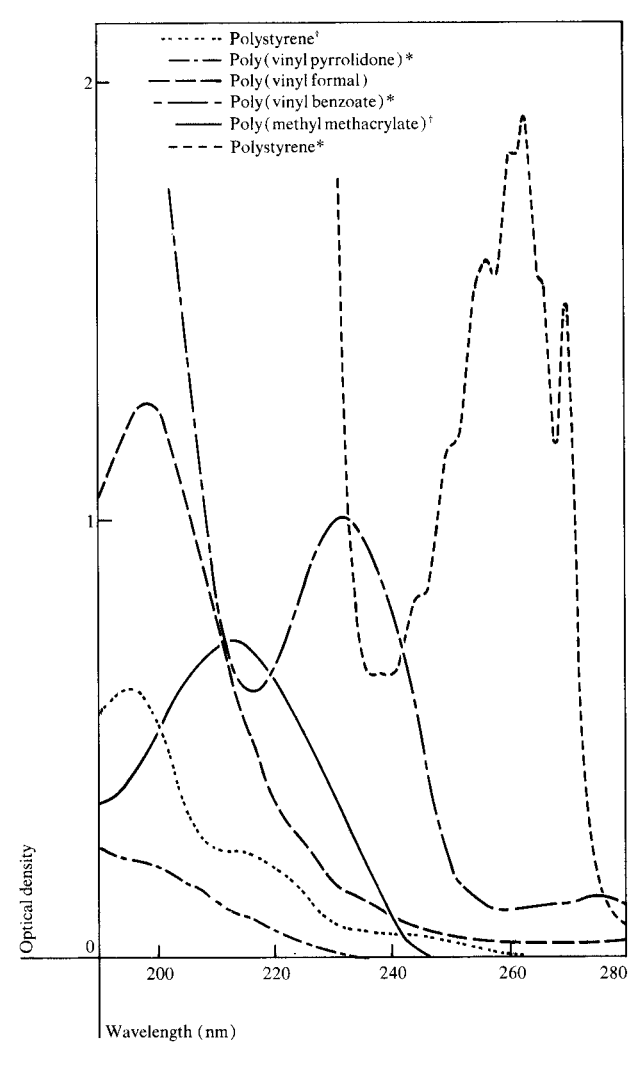


Figure 9 Optical density of some polymer films. The films \*, † are  $\approx 1~\mu m$ ,  $\ll 1~\mu m$  thick, respectively. The spectra of polyacrylonitrile and poly(vinyl alcohol) resemble that of poly(vinyl pyrrolidone). Poly(vinyl carbazole) shows very low structured absorption between 350 and 190 mm, and therefore their spectra are not shown.

Poly(vinyl-formal)\* - - Polystyrene\*† - - - -, ---Poly(vinyl pyrrolidone)\* - - - --Poly(methyl methacrylate)† ---Poly(vinyl benzoate)\* - - - -

transforming them to a consistent coordinate system. Also, they pointed out that the local field may not be a Lorentz field. Nevertheless, the results are sufficiently accurate, even if lacking theoretical rigor, and they can be used to predict, approximately, refractive indices.

Copolymers [12] offer the opportunity to fabricate films of variable refractive index, which can be matched to the refractive indices of other polymeric materials. Since it is difficult to find compatible polymers in solution with widely differing indices, we have synthesized

copolymers. Thus, we have esterified poly(vinyl alcohol) with naphtoyl chloride to raise the index by 0.01. In selecting other ester substituents for a more significant change of  $\Delta n$ , a table relating molecular structure or functional groups with optical properties proves useful. Thus halogenated (except fluorinated) acids as well as unsaturated aliphatic or aromatic acid may be used as esterifying agents of poly(vinyl alcohol) (PVA), if an increase in  $\Delta n$  is desired. Conversely, trifluoroacetic acid or other fluorinated saturated aliphatic acids may be considered if a decrease in the  $\Delta n$  of PVA films is intended, e.g., for coatings on light guides [29].

#### Summary

Even though other methods for determining the optical properties of thin organic films exist [30], we have found the use of integrated optics to be a very convenient and accurate method. As a result, we have readily measured refractive indices including anisotropies, absorptions and film thicknesses for a number of polymeric films

### **Acknowledgments**

We wish to thank R. C. Guarnieri and J. Pinto for making the sputtered glass films and J. Bargon and F. L. Rodgers for the synthesis of the copolymers.

#### References

- IEEE Trans. Microwave Theory Tech. MTT-23 (January 1975). (Special issue on integrated optics and optical waveguides.)
- 2. S. E. Miller, IEEE J. Quantum Electron. QE8, 199 (1972).
- 3. Introduction to Integrated Optics, edited by M. K. Barnoski, Plenum Press Inc., New York 1974.
- F. Zernike, "Fabrication and Measurement of Passive Components," in *Integrated Optics*, edited by T. Tamir, Springer-Verlag, New York 1975, Ch. 5.
- E. M. Zolotov, V. A. Kiselev, and V. A. Sychugov, Soviet Phys. Usp. 17, 64 (1974).
- Y. Suematsu, Y. Sasaki, E. Asai, M. Hakuta, and H. Noda, Electron. Commun. Jap. 55, 82 (1972).
- 7. R. Ulrich and R. Torge, Appl. Opt. 12, 2901 (1973).
- 8. R. Th. Kersten, Optics Commun. 9, 427 (1973).
- 9. R. Th. Kersten, Optics Commun. 13, 327 (1975).
- 10. D. J. Walter, Thin Solid Films 23, 153 (1974).
- J. D. Swalen, M. Tacke, R. Santo, and J. Fischer, Optics Commun. 18, 387 (1976).
- 12. V. Ramaswamy and H. P. Weber, *Appl. Opt.* 12, 1581 (1973).
- J. Fischer, R. Santo, and J. D. Swalen have produced films of these materials.
- P. K. Tien, G. Smolinsky, and R. J. Martin, Appl. Opt. 11, 637 (1972).
- 15. P. K. Tien, G. Smolinsky, and R. J. Martin, *IEEE Trans. Microwave Theory Tech.* MTT-23, 79 (1975).
- P. K. Tien, R. J. Martin, and G. Smolinsky, Appl. Opt. 12, 1909 (1973).
- M. J. Vasile and G. Smolinsky, J. Electrochem. Soc. 119, 451 (1972).
- L. F. Thompson and G. Smolinsky, J. Appl. Polymer Sci. 16, 1179 (1972).
- 19. J. Kane and H. Osterberg, J. Opt. Soc. Am. 54, 347 (1964).

- 20. P. K. Tien and R. Ulrich, J. Opt. Soc. Am. 60, 1325 (1970).
- 21. D. Marcuse, *Theory of Dielectric Optical Waveguides*, edited by Yoh-Han Pao, Academic Press, New York 1974.
- H. Kogelnik, "Theory of Dielectric Waveguides," in *Integrated Optics*, edited by T. Tamir, Springer-Verlag, New York 1975, Ch. 2.
- 23. T. Tamir, "Beam and Waveguide Couplers," in *Integrated Optics*, *ibid.*, Ch. 3.
- J. N. Polky and G. L. Mitchell, J. Opt. Soc. Am. 64, 274 (1974).
- 25. R. H. Partridge, J. Chem. Phys. 47, 4223 (1967).
- N. A. Lange, Handbook of Chemistry, Handbook Publishers Inc., Sandusky, OH, 1949, p. 1052.
- 27. K. Pitzer, Adv. Chem. Phys. 2, 59 (1959).
- W. J. Mills, "Optical Properties," in *Polymer Science*, edited by A. D. Jenkin, North Holland Publishing Co., Amsterdam 1972, Ch. 7.
- 29. H. Dislich and A. Jacobsen, Abstr. XXIIIrd Int. Symposium on Macromol., Madrid, 1974, Vol. II, p. 787.
- O. S. Heavens, Optical Properties of Thin Solid Films, Dover Publications Inc., New York 1965, pp. 96-154.
- 31. R. Ulrich and H. P. Weber, Appl. Opt. 11, 428 (1972).
- 32. D. Hornauer and H. Raether, Optics Commun. 7, 297 (1973).

- 33. H. P. Weber, W. J. Tomlinson, and E. A. Chandross, *Opt. Quantum Electron.* 7, 465 (1975).
- T. P. Sosnowski and H. P. Weber, Appl. Phys. Lett. 21, 310 (1972).
- P. K. Tien, R. J. Martin, and S. Riva-Sanseverino, Appl. Phys. Lett. 27, 251 (1975).
- 36. F. Mohring, D. Volkmann, and D. Huhn, Opt. Quantum Electron. 7, 443 (1975).

Received April 28, 1976; revised October 19, 1976

J. D. Swalen and R. Santo are located at the IBM Research Division laboratory, 5600 Cottle Road, San Jose, California 95193; M. Tacke is located at the University of Würzburg, West Germany; and J. Fischer is located at the Ciba Geigy Corporation, Basel, Switzerland.